Bulletin of the Seismological Society of America. Vol. 48, pp. 133–146. April 1958

MECHANISMS OF THE AFTERSHOCKS OF THE KERN COUNTY, CALIFORNIA, EARTHQUAKE OF 1952

By Markus Båth and Charles F. Richter

ABSTRACT

Using directions of first motion of longitudinal waves recorded at near-by stations, the orientation of fault traces and the nature of fault motions have been deduced for fifty-seven earthquakes of the Kern County aftershock series. Unlike the main shock, the aftershocks exhibit considerable strike slip with left-hand strike slip dominating on and to the south of the White Wolf fault and right-hand strike slip and dip slip to the north of it. The two last-mentioned mechanisms represent a secondary strain release, beginning not earlier than thirty-seven hours after the main shock.

1. Introduction

Earlier studies of faulting mechanism in southern California by means of seismograms have been made by Gutenberg (1941), using first motions of longitudinal waves, and by Dehlinger (1952), using shear-wave vibrational directions. For the main Kern County earthquake on July 21, 1952, a solution was given by Gutenberg (1955*b*) by means of longitudinal and transverse waves at near and distant stations. The result was a fault plane dipping 60° to 66° toward E 50° S and a slip directed upward and northeastward in the southeastern block relative to the northwestern block. The dip-slip component was about 1.4 times the strike-slip component. In the present paper we shall investigate the mechanism for a number of the Kern County aftershocks as a contribution to an understanding of the mechanics of the whole system.

2. Observational Data

The observations of the direction of initial motion of the P waves are given in table 1 for fifty-seven aftershocks selected from Richter's (1955) list, including all of magnitudes $\geqq 5.0$ and a number of smaller shocks of special interest.

The following notation is used:

No. = shock number, assigned by Richter (1955)
M = magnitude
C = compression
D = dilatation
dC = small dilatation followed by large compression
cD = small compression followed by large dilatation
( ) = questionable reading; if no parenthesis is given, the reading is very clear
— = beginning gradual with indefinite direction, or obscured
Blank entry means that no record exists or that it has not been available for inspection.

The following abbreviations are used for the stations (see Gutenberg, 1955*a*, concerning location and instrumentation):

P = Pasadena, MW = Mount Wilson, R = Riverside, Pr = Palomar, LJ = La Jolla, SB = Santa Barbara, CL = China Lake, H = Haiwee, T = Tinemaha, BB = Big Bear, Bt = Barrett, Ch = Chuchupate, By = Berkeley, MH = Mount Hamilton, PA = Palo Alto, F = Fresno, M = Mineral, BC = Boulder City, Ro = Reno.

Manuscript received for publication March 18, 1957.

TABLE 1

OBSERVATIONAL DATA

No.	Date, time (G.C.T.)	Lat., long.	M	P	MW	R	Pr	LJ	SB	CL	H	T
	1952	deg. min.										
40	July 21	35 14	5.1	(C)	—	—	—	—	—	(cD)	D	D
	17:43	118 32										
46	July 21	35 08	5.5	C	—	C	C	—	C	D	D	D
	19:41	118 46										
58	July 22	35 12.5	4.4	C	—	(D)	—	—	(dC)	(C)	—	(D)
	03:21	118 37.5										
59	July 22	34 52	4.1	D	—	C	C	—	cD	(D)	—	dC
	07:45	118 52										
60	July 22	35 05	4.4	C	C	(C)	cD	—	D	D	(c)D	—
	08:16	118 35										
61	July 22	35 00	4.1	C	(c)D	—	C	—	(D)	C	—	cD
	08:21	119 00										
62	July 22	35 05	4.7	D	(D)	D	dC	—	C	C	(C)	D
	08:48	118 45										
63	July 22	35 14	4.5	D	D	—	dC	—	dC	C	C	D
	09:10	118 36										
64	July 22	35 02	4.1	dC	—	—	cD	—	D	(C)	D	cD
	10:20	119 00										
65	July 22	35 03	3.8	D	D	—	—	—	—	—	—	—
	10:44	118 30										
66	July 22	35 00	4.8	D	D	(C)	dC	—	dC	C	(C)	D
	13:32	119 00										
68	July 22	34 54	4.3	D	(D)	—	(dC)	—	C	—	—	D
	14:30	119 03										
69	July 22	35 14	4.2	D	D	—	(dC)	—	C	C	C	D
	15:03	118 32										
70	July 22	35 00	4.1	D	—	—	C	—	C	C	—	(c)D
	17:53	119 00										
71	July 22	35 13	4.3	(C)	C	—	—	—	—	C	D	D
	19:09	118 28										
73	July 22	35 04	4.2	D	D	—	—	—	—	D	—	—
	21:02	118 46										
74	July 22	35 01.5	4.7	C	C	—	C	—	dC	C	(C)	C
	22:32	118 55.5										
75	July 23	35 22	6.1	C	—	—	—	—	C	C	(C)	D
	00:39	118 35										
76	July 23	35.0	4.4	—	—	—	—	—	C	—	—	—
	00:43	119.0										
77	July 23	35 22	4.6	D	D	—	(C)	—	C	C	dC	C
	00:48	118 35										

TABLE 1—*Continued*

BB	Bt	Ch	By	MH	PA	F	M	BC	Ro	Additional data	No.
—	—		cD	—	D	(D)		C			40
(C)	C		D	D	dC	D		C			46
—	(D)		(C)	—	—	D	—	—	—		58
—	(cD)		—	(C)	—	D	(D)	—	—	White Oak: D	59
cD	(C)		—	D	—	D	—	—	—		60
(c)D	—		—	—	—	D	—	—	(C)	White Oak: D	61
—	—		—	(C)	—	D	—	—	—		62
cD	(C)		D	cD	—	D	—	cD	—		63
—	C		—	—	—	D	(D)	—	—		64
cD	(cD)		—	—	—	D		—	—		65
C	—		(D)	D	(C)	D		—	D		66
—	—		—	—	—	D		—	—		68
—	—		(D)	(D)	—	(D)		—	—		69
—	—		—	—	—	—		—	—		70
(cD)	—		(D)	(c)D	—	—		C	—		71
—	—		D	(D)	—	C	—	—	—		73
C	—		—	D	—	C	—	—	—		74
—	—		D	D	D	D	—	C	D	Santa Clara: D	75
—	—		—	—	—	—	—	—	—		76
—	—		—	C	C	—	—	(C)	—		77

TABLE 1—*Continued*

No.	Date, time (G.C.T.)	Lat., long.	M	P	MW	R	Pr	LJ	SB	CL	H	T
	1952	deg. min.										
78	July 23 03:19	35 22 118 35	5.0	D	D	(D)	(D)	—	C	C	(d)C	C
79	July 23 03:49	35 17 118 33	4.7	D	(D)	(D)	C	—	—	C	dC	C
80	July 23 04:02	35 22 118 35	4.7	D	D	(D)	D	—	C	C	dC	C
81	July 23 05:46	35 23 118 34	4.7	(D)	D	—	cD	—	—	C	C	C
82	July 23 06:11	35 16 118 27	4.2	D	(D)	—	—	—	C	C	—	D
83	July 23 06:26	35 22 118 35	4.0	—	—	—	—	—	C	C	C	C
84	July 23 06:54	35 22 118 35	4.2	D	—	—	—	—	D	(C)	(C)	C
85	July 23 07:37	35 17 118 33	4.8	D	D	—	D	—	dC	C	dC	dC
86	July 23 07:53	35 00 118 50	5.4	D	D	cD	C	—	cD	C	(D)	D
87	July 23 09:39	35 15 118 29	4.2	D	D	(D)	—	—	C	C	D	(dC)
88	July 23 10:54	35 19 118 30	4.1	D	D	—	cD	—	(C)	C	D	D
89	July 23 13:17	35 13 118 49	5.7	C	(c)D	C	C	—	C	D	D	D
97	July 23 18:14	35 00 118 50	5.2	C	D	D	D	—	dC	C	dC	dC
113	July 25 07:04	35 24 118 35	4.1	C	—	(C)	—	—	—	C	C	D
115	July 25 13:13	35 19 118 30	5.0	D	D	cD	cD	—	—	D	D	D
116	July 25 14:35	35 08 118 46	4.4	D	(cD)	D	(D)	—	(C)	C	—	D
117	July 25 19:10	35 19 118 30	5.7	D	D	D	(D)	—	dC	C	D	D
118	July 25 19:43	35 19 118 30	5.7	D	—	C	C	—	C	C	D	D
119	July 25 20:06	35 19 118 30	4.8	—	—	—	—	—	—	—	D	D
120	July 26 01:02	35 19 118 30	4.2	D	(D)	C	C	—	D	D	cD	D

TABLE 1—*Continued*

BB	Bt	Ch	By	MH	PA	F	M	BC	Ro	Additional data	No.
D	D		C	C	(C)	C	—	C	D		78
—			(dC)	(C)	—	D	—	C	—		79
D	—		—	C	—	D	—	C	—		80
(dC)	(D)		(C)	—	—	—	—	—	—		81
C	D	C	D	C	—	—	—	C	—		82
—	—		—	C	—	—	—	(C)	—		83
—	—		—	—	—	—	—	C	—		84
dC	D		—	D	—	D	—	C	—		85
—	C		eD	C	—	D	—	C	—		86
eD	—		—	D	—	D	—	(C)	—		87
—	eD		C	—	—	—	—	C	(D)		88
C	C		—	C	—	D	D	(D)	D		89
D	D		D	C	D	C	—	C	—	Dalton: (D)	97
—	—		(e)D	D	(C)	D	—	C	—		113
(e)D	(D)	C	eD	(eD)	(C)	(D)	(C)	eD	D		115
—	D	C	—	—	—	D	(D)	(C)	—		116
(C)	(D)	C	C	—	C	(D)	—	C	D	Santa Clara: dC	117
—	C	C	C	C	C	C	(C)	C	D		118
—	—	D	—	D	(D)	D	D	C	—		119
C	(eD)		—	(D)	—	—	—	—	—		120

TABLE 1—*Continued*

No.	Date, time (G.C.T.)	Lat., long.	M	P	MW	R	Pr	LJ	SB	CL	H	T
	1952	deg. min.										
140	July 29 05:56	35 23 118 51	3.9	C	C	C	(C)	—	(d)C	(c)D	—	C
141	July 29 07:04	35 23 118 51	6.1	C	C	C	C	C	C	D	C	C
142	July 29 07:56	35 23 118 46	3.8	(D)	—	dC	(dC)	—	—	C	—	C
143	July 29 08:02	35 24 118 49	5.1	D	D	D	D	—	C	C	dC	C
144	July 29 08:08	35 26 118 47	3.8	D	D	D	D	—	C	C	C	C
155	July 31 12:09	35 19.5 118 36.5	5.8	D	D	D	D		—	C	cD	D
161	Aug. 1 13:05	34 54 118 57	5.1	D	D	C	C		dC	C	C	(D)
177	Aug. 10 19:44	35 00 119 00	4.1	C	—	C	C		D	D	D	cD
194	Aug. 22 22:41	35 20 118 55	5.8	C	C	C	C		C	D	C	C
216	Sept. 12 10:35	35 00 119 03	4.5	C	(C)	C	C		(c)D	D	D	cD
241	Nov. 7 08:56	35 00 119 05	4.6	C	(D)	C	(C)		D	D	D	(c)D
	1953											
266	May 25 03:24	35 00 119 01	4.8	D		C			C	C	D	
275	Dec. 15 12:45	35 13 118 49	4.6	C	C		C			—	D	
	1954											
276	Jan. 12 23:34	35 00 119 01	5.9	C	—	C			D	C	D	D
279	Jan. 27 14:20	35 09 118 38	5.0	D	D	C			D	D	D	D
281	Feb. 7 00:10	35 02 119 06	4.4	C	C	C	C		D	D	D	cD
285	May 23 23:53	34 59 118 59	5.1	C	C	C	C		dC	D	D	—

TABLE 1—*Continued*

BB	Bt	Ch	By	MH	PA	F	M	BC	Ro	Additional data	No.
dC	C	D	—	—	—	D	—	—	—		140
D	D		D	D	D	D	—	D	dC		141
—	C		—	(C)	—	—	—	—	—		142
D	D	D	D	D	—	D	—	C	—		143
(dC)	dC	D	—	C	—	—	—	—	—		144
C	D	C	D	D	D	D	D	C	D	Dalton: (C), Tucson: C	155
C	—		D	D	—	D	—	—		Dalton: (C)	161
—	C									Woody: D, Havilah: C	177
C		D	D	D	C	cD	—		cD	Dalton: (D), Woody: C	194
C		C									216
C										Dalton: (D)	241
	D									Woody: D, Fort Tejon: C	266
	C									Fort Tejon: D, King Ranch: C	275
C	D									King Ranch: C, Isabella: (C)	276
C	C									Woody: D, Fort Tejon: C, Isabella: C	279
—	C									Woody: (D), Fort Tejon: D, Dalton: D	281
C	C									King Ranch: D, Isabella: D	285

The following locations were not included in Gutenberg's (1955*a*) paper:

Isabella, 35° 39′ N, 118° 29′ W; Reno (Nevada), 39° 32′ N, 119° 49′ W; Boulder City (Nevada), 35° 59′ N, 114° 50′ W; Tucson (Arizona), 32° 15′ N, 110° 50′ W.

Practically all the observations in table 1 were obtained by new readings from all available seismograms, and earlier lists, e.g., of Richter (1955, p. 196), were checked.

3. Methods

Plotting the observations for a given station on a map of the aftershock area, we find an apparently very irregular pattern with no possibility of separating areas giving compressions from those giving dilatations. Frequently, significantly opposite motions are obtained from the same epicenter. This is in sharp contrast to the usually regular distribution of initial motion obtained in studies of distant earthquake areas (see, e.g., Båth, 1952). A probable reason is that in the present study we are concerned with shocks of usually much lower magnitude than that for distant shocks. The weaker shocks may be expected, especially in an aftershock series, to occur on a large number of minor and auxiliary faults oriented in a variety of directions, whereas larger shocks are assumed to occur on the larger faults which conform better to the regional stress pattern. The complication from the fact that the first motion at nearer stations refers to the direct longitudinal wave (p), at more distant stations to the longitudinal wave refracted twice at the Mohorovičić boundary (Pn), is insufficient as an explanation, because the irregularity mentioned is observed at all stations, including those with only Pn observations.

In view of the mechanical complexity of the aftershock area, it was necessary first to study each shock individually. This was done by plotting the observations for each shock separately, with the epicenter at the origin and station azimuth and distance as polar coördinates. A modified technique mainly for distant observations was recently developed by Båth (1958), and the ideas expressed there may easily be transferred to the present representation, which is better when only observations of near stations are used. In each case nodal lines were drawn, i.e., lines separating compressional areas from dilatational (or lines of zero amplitude for the P waves). It is obvious that the nodal lines are the intersections (FF and MM respectively) of the earth's surface with the fault plane and with a plane perpendicular to the direction of slip.

We use the following notation:

a_F, a_M = the perpendicular distances from the epicenter E to FF and MM respectively

γ_F, γ_M = the respective dips of the fault plane and of the plane perpendicular to slip

α = the angle between FF and MM

β = the angle in the fault plane between dip and slip

h = the focal depth

The following relations hold, assuming rectilinear slip on a plane fault surface:

$$\tan \gamma_F = h/a_F ; \qquad \tan \gamma_M = h/a_M$$

$$\cos \alpha = \cot \gamma_F \cdot \cot \gamma_M ; \qquad \cos \beta = \cos \gamma_M / \sin \gamma_F$$

$$h = (a_M a_F / \cos \alpha)^{\frac{1}{2}}$$

The different special cases are as follows:

1. Strike slip:
   - A. Vertical fault: $a_F = 0; a_M = 0; \alpha = 90°$.
   - B. Horizontal fault: $a_F = \infty; a_M = 0; \alpha$ indeterminate.
   - C. Inclined fault: $a_F \neq 0, \infty; a_M = 0; \alpha = 90°$.
2. Dip slip:
   - A. Vertical fault: $a_F = 0; a_M = \infty; \alpha$ indeterminate.
   - B. Horizontal fault: excluded.
   - C. Inclined fault: $a_F \neq 0, \infty; a_M \neq 0, \infty; \alpha = 0°$. The distance between FF and MM in this case is $a_F + a_M = 2h/\sin 2\gamma_F$.
3. Combined slip:
   - A. Vertical fault: $a_F = 0; a_M \neq 0, \infty; \alpha = 90°$.
   - B. Horizontal fault: excluded.
   - C. Inclined fault: $a_F \neq 0, \infty; a_M \neq 0, \infty; \alpha \neq 0°, 90°$. This is the most general case.

Applying these considerations to our case, we find that for h as low as 16 km. the station net needs to be much closer in order to permit detection and determination of a_F, a_M. The nodal lines FF and MM can often be displaced parallel to themselves and still satisfy the observations as well as when they pass through E. Therefore it is impossible to make complete fault-plane solutions in the present case.

In our study we can only distinguish three types:

a. Uninodal type, i.e., 1B, 2A, or 2C above, usually 2C, whereas 1B seems to be excluded in our study. In fact, 2C may be considered as a binodal parallel type.

b. Binodal perpendicular type, i.e., 1A, 1C, or 3A.

c. Binodal nonperpendicular type, i.e., 3C.

In addition, we have to consider the complication from the fact that at the nearer stations the first longitudinal wave is p, and at more distant stations Pn. This was pointed out by Wadati (1927) and extensively developed by Kawasumi (1934). With the notation

H = the crustal thickness down to the Mohorovičić boundary
v_1 = the longitudinal wave velocity in the crust
v_2 = the longitudinal wave velocity immediately below the crust
i = the angle of incidence, defined by $\sin i = v_1/v_2$

we find the following expression for the critical distance Δ_c, where p and Pn arrive simultaneously, neglecting the earth's curvature:

$$\Delta_c = (2H - h) \tan i \left[1 + \left(1 + \frac{4H(H - h)}{(2H - h)^2 \tan^2 i}\right)^{\frac{1}{2}}\right]$$

For distances $\Delta < \Delta_c$ the first wave is p, and for $\Delta > \Delta_c$ it is Pn. It is to be noted that Δ_c is not necessarily the same in all directions from the epicenter, mainly owing to variations in H. Combining the Δ_c — formula with the earlier considerations, it is an easy matter to construct the theoretical distribution of initial motion under different circumstances.

In spite of the fact that the observations are insufficient to give complete solutions, they nevertheless usually define the directions of the nodal lines, one of which represents the fault trace, and they give the direction of the dominant motion.

TABLE 2

SOLUTIONS

No.	Uni-nodal	Bi-nodal	Φ	Motion	Exceptions	Remarks
			deg.			
40	×		48	sd	———	Two solutions offered, the uninodal possibly slightly better, considering Pasadena
		×	38	l	———	
46	×		66	sd	———	
58		×	65	r	———	
59		×	51	l	———	Case 1C
60	×		51	sd	———	
61		×	57, 132	r	Fresno	Case 3C
62		×	44	l	———	
63		×	17	l	———	
64		×	58	l	———	
65		×	(50)	l	———	
66		×	30	l	———	
68		×	33	l	———	
69		×	10	l	———	
70		×	46	l	———	
71	×		38	sd	———	
73		×	67	r	———	Case 1C
74		×	53, 113	r	Mt. Hamilton	Case 3C
75	×		50	sd	———	
76						Too few observations
77	×		(43)	su	———	First motion could be p at China Lake
78	×		80	su	———	Possibly case 2C
79		×	(80)	r	Palomar	Φ could be as large as 95°
80		×	(80)	r	Mt. Hamilton	Φ could be as large as 95°
81		×	(84)	r	———	Φ could be as large as 98°
82		×	44	l	———	
83		×	80	r	Mt. Hamilton	Two solutions offered
	×		(80)	su	———	First motion could be p at Santa Barbara in second case, or case 2C could give the solution
84	×		(80)	su	———	
85		×	36	l	———	
86		×	43, 145	l	———	Case 3C
87		×	32	l	———	
88		×	45	l	———	
89	×		(80)	sd	Mt. Hamilton	
97		×	60	r	Mt. Hamilton, Boulder City	Some indication of a double motion (possibly two shocks after each other), which could also explain the exceptions
113	×		18	sd	———	
115		×	59	l	———	Possibly case 1C
116		×	14	l	———	
117		×	45	l	Chuchupate	

TABLE 2—*Continued*

No.	Uni-nodal	Bi-nodal	Φ	Motion	Exceptions	Remarks
			deg.			
118		×	31, 158	l	———	Case 3C
119		×	38	l	———	
120		×	60	l	———	
140		×	43	r	Chuchupate, Fresno	
141		×	53	r	Barrett	Case 3A
142		×	63, 130	r	———	Case 3C; no reliable solution possible
143		×	(83)	r	———	Case 3A
144	(×)		(70)	su	Santa Barbara	Solution uncertain
155		×	40	l	———	Case 1C
161		×	44	l	Haiwee	The exception could be eliminated, assuming case 3C, giving Φ = 16° and 134°
177		×	(80)	l	Havilah	
194		×	49	r	Palo Alto, Big Bear, Chuchupate	
216		×	15	r	———	
241		×	(62)	l	———	Φ could be as large as 102°
266		×	46	l	———	
275		×	72	l	———	
276		×	50	l	———	
279		×	60	l	Fort Tejon, Isabella	
281		×	35	r	———	
285	×		54	sd	———	

4. Results

The solutions are compiled in table 2. "Binodal" means perpendicular binodal, unless otherwise mentioned. The following notation is used:

Φ = the angle in the horizontal plane between the meridian and a nodal line, measured from N over E; in the binodal perpendicular case only the smallest Φ is given; (Φ) indicates that Φ may be in error by more than 10°, otherwise Φ is accurate to within 5°–10°

r = right-hand strike slip

l = left-hand strike slip, both r and l referring to the direction Φ

su = southeast side moves upward

sd = southeast side moves downward

Only significant exceptions are given in table 2. They may be due:

i) to occurrence of p instead of Pn for the nearest stations,

ii) to situation close to a nodal line,

iii) to unknown reversals of the connections of seismometer to galvanometer.

The nodal lines have been drawn so as to give a minimum number of exceptions.

The results are shown on a map, figure 1, where usually only those nodal lines have been chosen which are most nearly parallel to the main fault, assuming these nodal lines to represent FF.

In contrast to the dominating dip slip in the main earthquake, strike slip predominates in the aftershocks. On the main White Wolf fault and to the south of it, left-hand strike slip dominates in conformity with the general motion pattern of the whole region (Benioff, 1955*b*, fig. 2). North of the main fault, on the other hand, the motion is almost exclusively right-hand strike slip or dip slip. We interpret this as a secondary or auxiliary release of strain, caused by the dominant left-hand

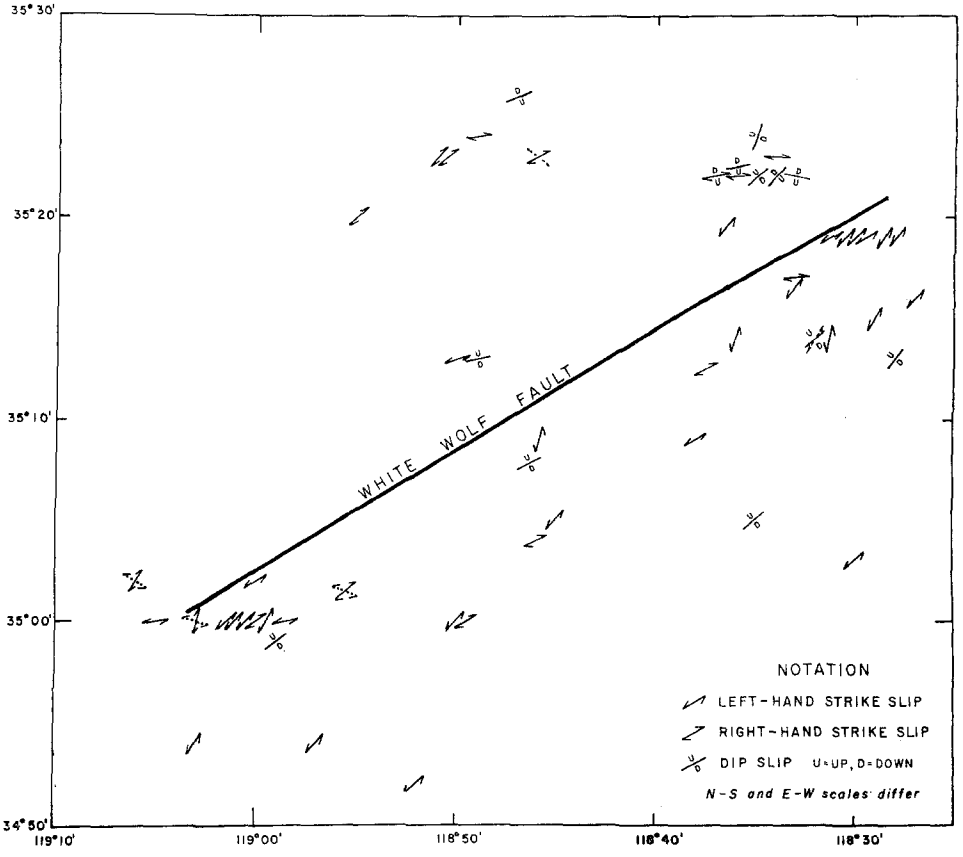

Fig. 1. Map of the aftershock area showing the individual solutions.

strike slip. The left-hand strike slip on the main fault will give rise to a strain pattern, which at some distance from the fault will be released as a right-hand strike slip. This secondary release could be expected on either side of the main fault; in the present case the secondary release occurred only on the northern side. In this connection it is of interest to note that there was a delay in the release on the northern side of thirty-seven hours after the great shock. After that time both mechanisms were in operation simultaneously, causing a change of the total strain release thirty-seven hours after the main earthquake (Benioff, 1955*a*). This occurrence was covered before and after by studying shocks nos. 58–89 inclusive. The second phase in the strain-release curve began with no. 75, initiating the activity around 35° 22′ N, 118° 35′ W, with right-hand strike slip and dip slip. These shocks also exhibit a different appearance on the records.

The two exceptions with left-hand strike slip on the northern side, i.e., nos. 155 and 275, are both located closer to the main White Wolf fault. No. 155 is also exceptional in originating at greater depth (around 23 km.) than the majority of the aftershocks, which occurred around 16 km. depth. No. 275 is of interest because, like no. 89, it is situated within an area of considerably reduced activity immediately north of the main fault.

Aftershocks with dominating dip-slip motion are in the minority but occur in most parts of the aftershock area. It is of interest to note that, unlike what occurred at the time of the main shock, the southeastern side usually has a downward motion relative to the northwestern side. Exceptions occur only in the limited area around 35° 22′ N, 118° 35′ W, initiated by no. 75.

On July 25, 1952, a series of shocks occurred around 35° 19′ N, 118° 30′ W, near the northeastern end of the active fault (nos. 115, 117–120) at an approximate depth of only 10 km. These shocks exhibit exclusively a dominating left-hand strike slip, agreeing with the main motion in the region, and consistent with the suggestion that they represent a terminal extension of the original faulting.

A series of shocks on July 29, 1952, i.e., nos. 140–144, near 35° 23′ N, 118° 50′ W are of special interest because, although belonging to a very limited area, they showed definitely opposite initial motions at some stations though not at others. It is clear from the map that these apparently contradictory cases fit very well into a coherent motion pattern with right-hand strike slip. The reversals of motion at several stations are attributable to somewhat different orientation of the faults in the different cases.

Several shocks were studied because of their location near the epicenter of the main earthquake at 35° 00′ N, 119° 02′ W. This group includes nos. 61, 64, 66, 70, 76, 177, 216, 241, 266, 276, 281, and 285. With dominating left-hand strike slip it is obvious that they generally do not agree with the mechanism of the main shock. No. 216 and no. 281 have been given with both nodal lines indicated, since it is not immediately obvious which of them is to be interpreted as FF. No. 281 (February 7, 1954) is of interest as representing a possible extended faulting northwestward from the southwestern end of the White Wolf fault, which took place late in the series, probably beginning on January 12, 1954.

Two examples of approximately opposite motions in almost the same place are offered by nos. 62 and 73 and by nos. 86 and 97, in each pair the left-hand strike-slip motion corresponding to that occurring in the earlier shock.

The Walker Pass earthquakes of 1946 (Chakrabarty and Richter, 1949) have possibly some mechanical relation to the Kern County series. The first motions of longitudinal waves for the large foreshock and the main earthquake indicate a binodal perpendicular solution with $\Phi = 35°$ and left-hand strike slip, thus agreeing with the main regional motion pattern. The orientation $\Phi = 35°$ of FF is of interest, since it nearly coincides with the trend of the aftershock area and other structural features (*loc. cit.*, fig. 1), thus indicating the existence of a fault with this direction; this could be the major front fault of the Sierra Nevada, with moderately steep westward dip.

References

Båth, M.

1952. "Initial Motion of the First Longitudinal Earthquake Wave Recorded at Pasadena and Huancayo," *Bull. Seism. Soc. Am.*, Vol. 42, No. 2, pp. 175–195.

1958. "Polar Graphs of Initial Motions at an Earthquake Source," *Bull. Seism. Soc. Am.*, Vol. 48, No. 2, pp. 129–131.

Benioff, H.

1955*a*. "Mechanism and Strain Characteristics of the White Wolf Fault as Indicated by the Aftershock Sequence," California Division of Mines, *Bull.* 171, pp. 199–202.

1955*b*. "Relation of the White Wolf Fault to the Regional Tectonic Pattern," *ibid.*, pp. 203–204.

Chakrabarty, S. K., and C. F. Richter

1949. "The Walker Pass Earthquakes and Structure of the Southern Sierra Nevada," *Bull. Seism. Soc. Am.*, Vol. 39, No. 2, pp. 93–107.

Dehlinger, P.

1952. "Shear-wave Vibrational Directions and Related Fault Movements in Southern California Earthquakes," *Bull. Seism. Soc. Am.*, Vol. 42, No. 2, pp. 155–173.

Gutenberg, B.

1941. "Mechanism of Faulting in Southern California Indicated by Seismograms," *Bull. Seism. Soc. Am.*, Vol. 31, No. 4, pp. 263–302.

1955*a*. "Seismograph Stations in California," California Division of Mines, *Bull.* 171, pp. 153–156.

1955*b*. "The First Motion in Longitudinal and Transverse Waves of the Main Shock and the Direction of Slip," *ibid.*, pp. 165–170.

Kawasumi, H.

1934. "Amplitude of Seismic Waves with the Structure of the Earth's Crust and Mechanisms of Their Origin," *Bull. Earthq. Res. Inst.*, Vol. 12, pp. 660–705.

Richter, C. F.

1955. "Foreshocks and Aftershocks," California Division of Mines, *Bull.* 171, pp. 177–197.

Wadati, K.

1927. "On the Mohorovičić Wave Observed in Japan," *Geophys. Mag.*, Vol. 1, pp. 89–96.

Seismological Laboratory,
California Institute of Technology,
Pasadena, California
(Division of Geological Sciences, contribution no. 826.)